JOURNAL OF MATERIALS SCIENCE 35 (2000) 2175–2183

Characterization and comparative study of three-dimensional braided hybrid composites

T. D. KOSTAR
Foster-Miller, Inc., Waltham, MA 02451-1016, USA
E-mail: tkostar@foster-miller.com

TSU-WEI CHOU
Center for Composite Materials and Department of Mechanical Engineering, University of Delaware, Newark, DE 19716, USA

P. POPPER
DuPont, Central Research and Development, Wilmington, DE 19880, USA

Cartesian three-dimensional braiding as a method of preforming for hybrid composites has been investigated. The fundamental case of a two-sided hybrid 3-D braid was chosen. Hybrid preforms, along with a corresponding set of non-hybrid preforms for control, were fabricated using a Cartesian braiding method. The preforms were consolidated through a Resin Transfer Molding process and prepared for characterization and mechanical testing. Characterization of the braided hybrid composite specimens included yarn packing and deformation within an assumed unit cell, and measurement of constituent tow fiber volume fraction using digital image analysis. A comparison study of the elastic performance of Kevlar/epoxy and carbon/Kevlar hybrid composites was carried out. The tension test results show a near-linear stress-strain relationship for both specimen types within the range of the applied load. The tensile modulus for the carbon/epoxy and hybrid composite were found to be 41 GPa and 74 GPa, respectively. In addition, the Poisson ratio of near unity for both specimen types strongly suggests a fiber dominated material response. The difference in hybrid composite transverse strain due to the differing constituent fiberous materials is found to be appreciable. It is believed that this discrepancy in Poisson contraction, between the carbon and Kevlar sides of the specimens, causes the propagation of transverse cracks [primarily within the carbon tows] and ultimately leads to catastrophic composite failure. Composite ultimate strength and strain to failure were found to be 793 MPa and 1.9% for the Kevlar/epoxy sample and 896 MPa and 1.1% for the carbon/Kevlar hybrid.

1. Introduction

The design and fabrication of preforms for advanced composites has gained considerable attention in light of the recent advancements in textile preforming techniques. It is within this realm of preforming technology that the full advantage of the knowledge of process-structure-property relations may be realized. The fabrication process of these preforms directly determines composite micro-structure and resulting mechanical properties. Textile preforms may be loosely classified into two-dimensional (2-D) and three-dimensional (3-D) structures, depending on the degree of reinforcement between layers [1]. These textile structures may be either stitched, knitted, woven, braided, or made by a combination of two or more forming methods. We start with some background on 3-D Cartesian braiding and the preforms thus formed.

1.1. Three-dimensional braiding

Three-dimensional braids are formed on two basic types of machines. These are the horngear and Cartesian machines which differ only in their method of yarn carrier displacement. While the horngear type machines offer improved braid speed over the Cartesian machines, the Cartesian machines offer compact machine size, comparatively low development cost, and braid architectural versatility.

Horngear machines with square or circular arrangement are employed in the fabrication of solid braids. Present-day machines are limited in size and shape of braidable preform. The micro-geometry of the braid is also restricted. The braider yarns form simple intertwined helical paths throughout the structure with little to no variation possible.

To allow for more flexibility in preform size, shape, and micro-structure, new braiding processes have

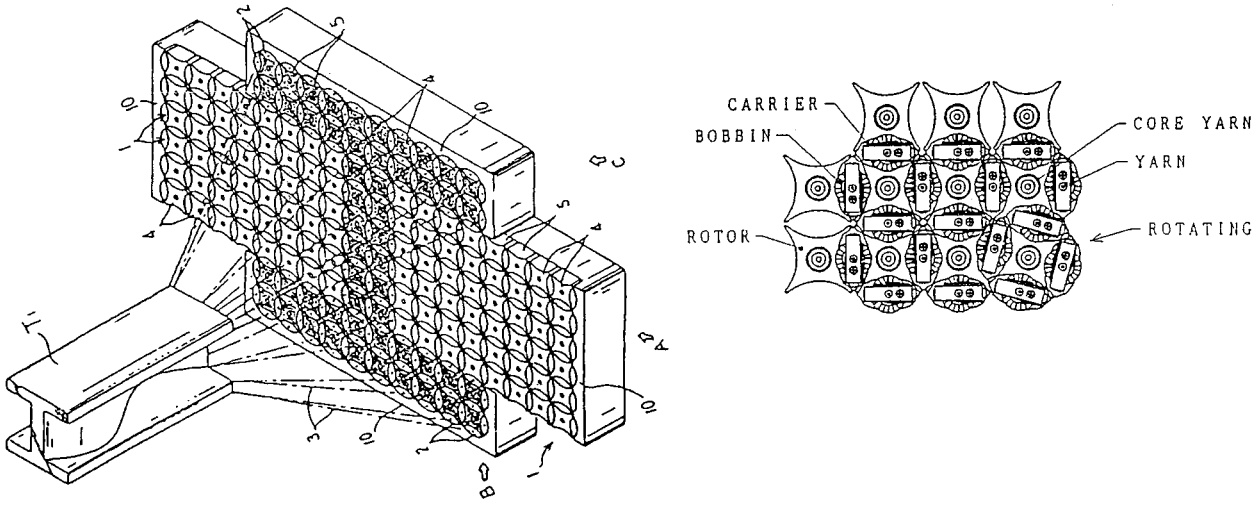

Figure 1 Advanced 3-D solid braiding [6].

been introduced. These include AYPEX [2], interlock twiner [3, 4], 2-step [5], 3-D Solid [6] (Fig. 1), and Cartesian [7] which is more commonly referred to as 4-step or track and column in the literature. A recent assessment of textile preforming methods has been conducted by Chou *et al.* [8]. Of all the 3-D braiding processes, the 3-D solid and Cartesian methods represent the apex of braiding technology. Since they differ mainly in approach to yarn carrier displacement (horngear vs. track and column), we need only to understand a single process in order to understand the architectures and structures which may be formed.

1.2. Cartesian braiding process

The basic Cartesian braiding process involves four distinct Cartesian motions of groups of yarns termed rows and columns. For a given step, alternate rows (or columns) are shifted a prescribed distance relative to each other. The next step involves the alternate shifting of the columns (or rows) a prescribed distance. The third and fourth steps are simply the reverse shifting sequence of the first and second steps, respectively. A complete set of four steps is called a machine cycle (Fig. 2). It should be noted that after one machine cycle the rows and columns have returned to their original positions. The braid pattern shown is of the 1×1 variety, so called because the relation between the shifting distance of rows and columns is one-to-one. Braid patterns involving multiple steps are possible but they require different machine bed configurations and specialized machines. This unique "multi-step" braiding technique is what renders Cartesian braiding a versatile process. Track and column braiders of the type depicted in Fig. 2 may be used to fabricate preforms of rectangular cross-section such as T-beam, I-beam, and box beam if each column and row may be independently displaced. Cartesian braided composites offer excellent shear resistance and quasi-isotropic elastic behavior due to their symmetric, intertwined structure. However, the lack of unidirectional reinforcement results in low stiffness and strength, and high Poisson effect. To help eliminate this, some advanced machines

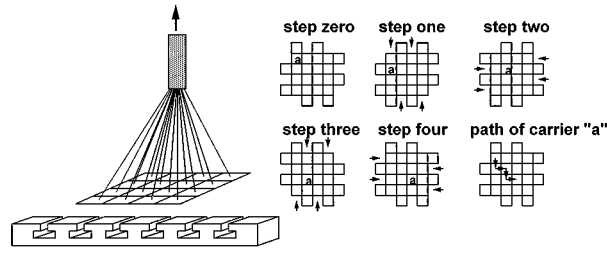

Figure 2 The Cartesian braiding process [7].

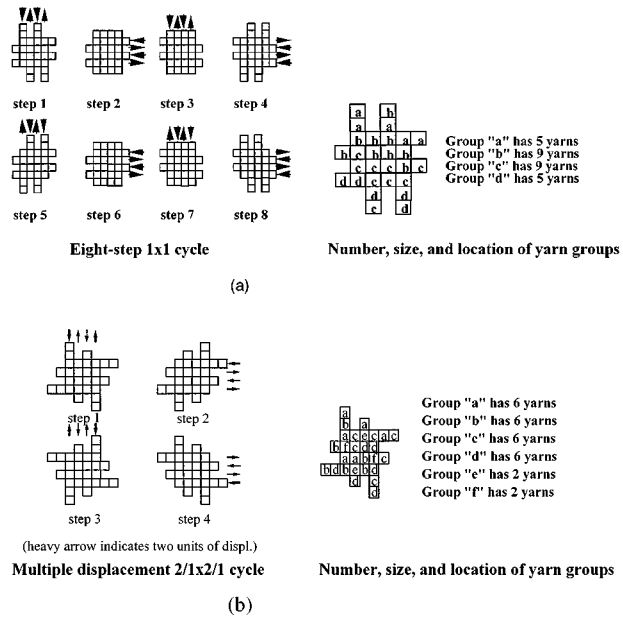

Figure 3 Example braid patterns employed in a multi-step braiding scheme. (a) A multi-step braid pattern where a complete cycle is made up of eight steps, and (b) a multiple displacement braid pattern which is utilized in the formation of hybrid structures [9].

allow axial yarns to be fed into the structure during fabrication.

As discussed above, the introduction of multiple step or multiple displacement braid patterns renders Cartesian braiding a versatile process. This extended 3-D braiding process, referred to as "multi-step" braiding in the literature [9], may be exemplified by the sample braid patterns shown in Fig. 3. This work focuses on a

single aspect of multi-step braiding. Namely, the selective grouping of yarns to form unique hybrid structures.

2. Specimen fabrication and preparation

Performance of hybrid braided composite members may be investigated so that the effects of drastic microstructural modifications such as hybridization are better understood. This work focuses on the characterization and comparative study of three-dimensional braided hybrid composites. As alluded to in Fig. 3, the formation of hybrid 3-D braids is a by-product of a phenomena known as yarn grouping.

2.1. Hybrid braid fabrication

The recent development of three-dimensional, multi-step braided composites has given birth to other exciting design possibilities. One of these design approaches is the grouping of yarns at a desired location in order to form a hybrid composite. Yarn groups are sets of yarn tows which travel the same path. A four-step braiding process will yield either one, two, or more yarn groups depending on factors such as the even/odd number of tracks and columns. In addition, these groups will always form in a symmetrically distributed pattern and contain the same number of yarns. However, a multi-step braiding process may have multiple yarn groups and a varying number of yarns per group. Different braiding schemes will yield different distributions of yarn groups. For example, certain track and column shifting sequences will group certain yarns near the sides or interior. This phenomenon has a direct application to hybrid composites where high performance yarns such as carbon may be placed only where needed.

The simplest and most fundamentally important grouping of yarns is that which occurs near a side. We state this for the following reason. The overlapping region of two orthogonal side areas is, in essence, a corner area. Therefore, by defining two orthogonal side areas, one can effectively define a corner area. Indeed, by defining all four side areas, the interior can be identified. For this reason, a thorough understanding of the side grouping phenomena will bear much fruit.

For example, consider a desired grouping of yarns in a particular side of a braided preform. We define this side as the entire upper half of the braid. We further require a minimum percentage of the yarns which start in this location to remain there, and following some fundamental rules [9], determine a machine cycle (i.e. track and column shifting sequence) which will yield the desired grouping. The result is the shifting sequence and corresponding yarn grouping shown in Fig. 4. Note that instead of a single group, three groups (a, b, c) comprise our desired yarn group. Finally, by demanding grouping on the top half we should expect, and indeed do, observe similar grouping occurring on the bottom half.

This simple case of a two-sided hybrid braid may now be investigated in order to quantify the effects of hybridization on mechanical performance. A series of carbon/Kevlar two-sided hybrid braids were fabricated,

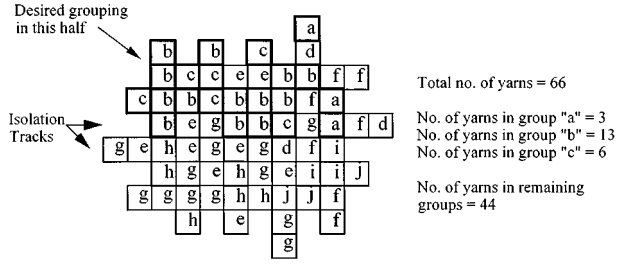

Figure 4 Example of side grouping of yarns to form a two-sided hybrid braid [9].

along with pure Kevlar fiber braids of the same architecture, and consolidated for characterization and mechanical testing.

2.2. Braid consolidation and preparation

The need to maintain composite dimensional uniformity dictates the use of RTM in the consolidation of tension test specimens. For the comparative performance study presented later, it was decided to use a preform which exhibits a two-sided yarn grouping with respect to its cross-section. Samples of the pure Kevlar and Carbon/Kevlar hybrid preforms are shown in Fig. 5 along with the four step braid cycle which was used to fabricate them. From Fig. 5, the slight variation from a four step 1×1 braid cycle, namely the double displacement of the two labeled opposing tracks, results in the observed grouping of yarns on the two halves of the preform cross-section. Since it was desired to maintain the 3-D elastic response of the final composite specimens, the preform cross-sectional dimensions differed from the ASTM suggested standard. For the given braid plan, a Celion Carbon tow denier of 4000 (0.024 in. dia.), and a Kevlar-49 denier of 5680 (0.029 in. dia.), the measured in-tension (on machine) dimensions of the braids were found to average 0.400 inches by 0.125 inches. While some researchers have locked-in the preform architecture by encasing the mold about the in-tension braid, it was decided that this approach would prove too time consuming. Instead, a mold was made where the braided composite dimensions were set at 0.435 inches by 0.135 inches. This allowed a near in-tension structure to be recaptured while making fabric insertion to the mold feasible. Fig. 6a shows a schematic of the fabricated mold. It should be noted that fabric compaction as a result of mold insertion is due to a predetermined deformation (mold dimensions) and not an applied force.

A standard RTM press set-up was used during resin injection. Fig. 6b shows a schematic of the main components of this rig. The epoxy resin system used was Epon Epoxy 862 with Epi-cure W curing agent. The resin was injected at near atmospheric pressure from a vacuum chamber and allow to wet-out the preform for approximately 20 minutes. Resin flow was then terminated and the manufactures suggested cure cycle of three hours implemented. After being allowed to cool to room temperature, the parts were de-molded. Fifteen specimens each of the pure Kevlar and Carbon/Kevlar hybrid preforms were consolidated in this way. Fig. 5b

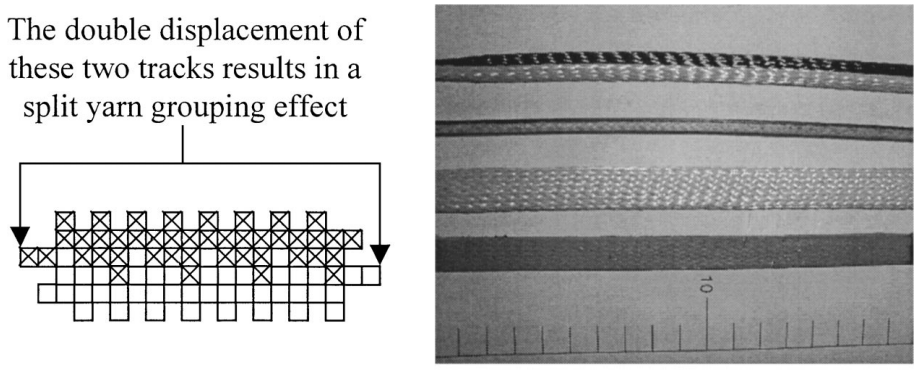

Figure 5 (a) Braid plan and (b) sample preform specimens that were consolidated through RTM (yarn elements marked with a × represent the location of carbon tows).

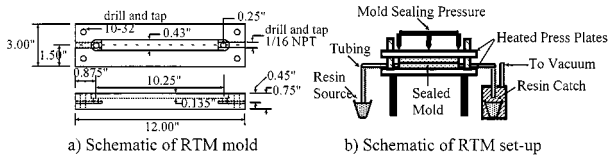

Figure 6 Schematics of mold and RTM set-up used for consolidation of the tension test specimens.

TABLE I Pertinent properties of the constituent materials used in this study [1, 9, 12 –14]

Property \ Material	Carbon (celion 4000)	Kevlar-49	Epon epoxy
Density (g/cc)	1.95	1.44	N/A
Tensile strength (MPa)	4000	3500	103
Tensile modulus (GPa)	235	127	3.45
Failure strain (%)	1.0	2.4	10.6
Poisson's ratio	0.28	0.3	0.35

shows a photograph of two of the finished samples side by side with the dry preforms. Table I supplies a list of the pertinent properties for the constituent materials used in this study.

Some observations have been made during the preparation of the composite specimens. First, preform deformation during mold insertion is inconsistent and, as a result, composite microstructure is not expected to be identical for each specimen. However, the high compaction of the fabric does insure near in-tension braid structure and fiber volume fraction. Second, after a difficult de-molding step, some composite warpage was observed. This occurred to a slightly larger degree in the Carbon/Kevlar hybrid composites. It is believed that two factors dominate this undesirable warpage effect. In its preform state, the braid is pre-stressed during mold insertion and this causes the small warpage of the pure Kevlar composites. This effect is compounded with the significant difference in stiffness and CTE of the fibers in the hybrid structure. As a result, a post-curing cycle was needed to help alleviate these residual stresses (80 degrees Celsius for 3 hours).

A total of 12 each of pure Kevlar and carbon/Kevlar hybrid composite samples were prepared for uni-axial (braid direction) tension testing. After the aforementioned post-curing to relieve residual stress and warpage, the inlet and outlet ends of the specimens were cut to remove unwanted resin material. End tabs of 3.81 cm (1.5 inch) lengths were then securely attached, leaving a specimen gauge length of 15.24 cm (6.0 inches). From the literature [10], it is suggested that a strain gauge size be selected such that its deformable length be greater than or equal to the unit cell size of the textile composite. This is to insure that strain gauge deformation corresponds to an average deformation across a representative unit of the braided composite microstructure. For the braided specimens in question, this size corresponds to the surface pitch length. After identifying an average pitch length of 0.381 cm (0.15 inches), a strain gauge size of 0.476 cm (0.1875 inches) (CEA-06-375UW-350, 2.08 gage factor, Measurements Group, Inc.) was chosen. Two gauges ($\times 2$ for the hybrid composites) were then securely fastened atop a representative surface unit cell in both the longitudinal and transverse directions. This attachment of gauges was repeated for each side (Kevlar and carbon) of the hybrid composites.

In order to study the microstructure of the braided composites, 1.9 cm (0.75 inch) lengths were cut from the consolidated specimens. These were then placed in cylindrical micrograph specimen holders and encased in Epo-Kwick^{TM} Resin (5 : 1 weight ratio to hardener). To obtain excellent resolution of the microstructures, a strict polishing procedure was adhered to. Each micrograph specimen was subjected to 180, 240, 320, 400, and 600 grit sand paper for a period of 3 minutes on a standard polishing apparatus. To further improve microstructure clarity, solutions containing 12.5, 9.5, and 5.0 micron Alumina particles were prepared and used in the final polishing steps.

3. Composite characterization

The characterization of braided composite microstructure may be investigated at two scales. The first is the yarn tow size and the second is the fiber (or filament) level. Braid packing during preforming and consolidation may be determined by a number of factors such as yarn tension, yarn twist, braid compaction, and molding pressure, injection pressure, resin viscosity, respectively.

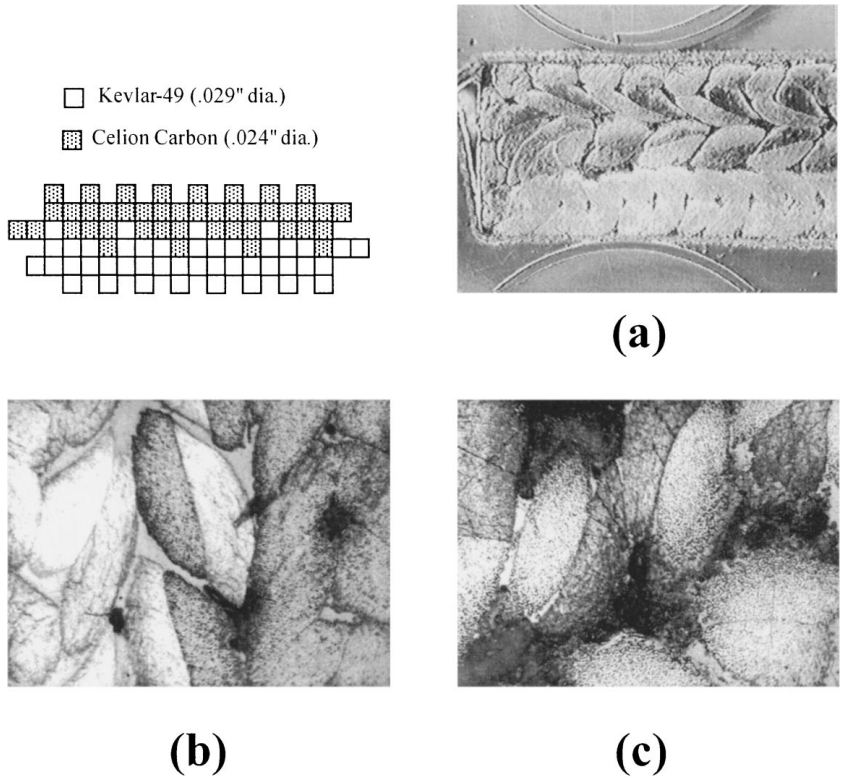

Figure 7 Cross-sectional microstructure of two-sided hybrid composite braids showing (a) the yarn packing and (b, c) yarn interaction between different tows.

3.1. Braid packing and yarn deformation

The packing of yarns within a four-step 1×1, non-hybrid braided composite is fairly well documented [11–14]. However, when one deals with a hybrid braided composite, the variation in braid microstructure may be significant. As an example, consider a microstructural cross-section of the the two-sided hybrid composites which have been consolidated through RTM (Fig. 7). The unique yarn paths which result from the yarn group producing braid cycle cause an un-orthodox yarn packing. A worthwhile goal would be to quantify this effect for a few select cases so that a basic understanding of yarn-to-yarn interaction and yarn cross-sectional deformation may be gained.

In Fig. 7, the fibers used to fabricated the hybrid structures are Kevlar-49^{TM} (0.029 in. dia. tow, approx. 35 micron fiber dia.) and Celion^{TM} Carbon (0.024 in. dia. tow, approx. 7 micron fiber dia.).

3.2. Fiber volume fraction

The calculation or measurement of braided composite fiber volume fraction is more readily obtain through the identification of a unit cell of the structure [1]. However, when dealing with multi-step, multiple fiber, and filler material braided composites, the identification of a unit cell is tedious. For this study, a possible representative cell for the sample braided composite microstructure is suggested. Focus is then on the measurement of the fiber volume fraction within the tows of the cell so that it may be quantitatively related to the aforementioned observed yarn packing.

The measurement of the yarn tow fiber volume fraction was carried out through use of digital image analysis. After a representative cell of the composite microstructure was chosen, a series of random image samples were picked from within the fiber bundles. These image samples were then thresholded. In other words, a gray-level value was chosen as a cut off such that all image pixels above and below this value were made white and black, respectively. The pixels in the resulting binary (black and white) image may then be counted and a ratio of white pixels (fibers) to total pixels (fibers and matrix) computed. Ideally, this ratio should represent the fiber volume fraction within the yarn tow. It should be noted that some error is introduced by this method due to such factors as image resolution and improper thresholding but it is believed to be a fairly accurate and straight forward one.

Fig. 8 shows the chosen representative cell for the two-sided hybrid composite. The measured fiber volume fractions for carbon and Kevlar are 74% and 64%, respectively. This rather high fiber volume fraction within the tows (packing fraction [15]) is comparable to that found in a four-step 1×1 braided composite [1, 16–18]. It should be noted that the high fiber volume fraction measured in this sample is likely due to the high braid compaction during RTM of the preform. The slightly greater fiber volume fraction of carbon over that of Kevlar may be attributed to the smaller fiber diameter (about 7 microns) compared to that for the Kevlar filaments (about 35 microns).

4. Performance study

The prediction of the elastic and strength properties of 3-D braided composites presents an interesting challenge. Although much progress has been made

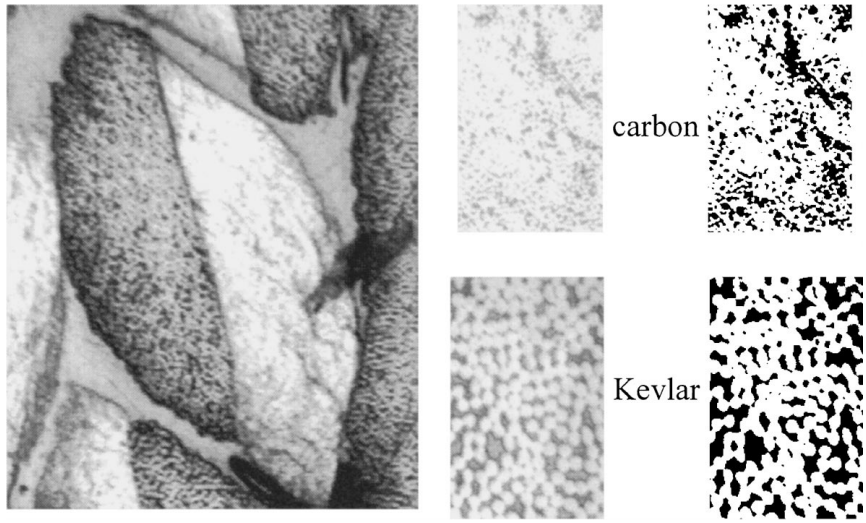

Figure 8 Measurements of fiber volume fractions within tows for the two side braided hybrid composite sample through digital analysis. The images on the right are the thresholded (binary) versions of their corresponding images from the left.

in this area [1, 12–14, 17–23], it is hoped that the study presented here with regards to the characterization and performance of hybrid braided composites may benefit the future modeling of mechanical properties. Our work is focused on the measured tensile response and hybridization effects of braided composites with the ultimate goal being the quantification of the dominant parameters involved in determining the composite elastic constants, strength, and fracture mechanism.

4.1. Comparison of tensile properties

Uni-axial tension tests were performed on the aforementioned prepared samples. The tensioning apparatus used was an Instron 1125 mechanical testing machine. Load was applied to the specimens by way of constant deformation which was, in turn, induced by a cross-head speed of 0.127 cm/min. (0.05 in./min.). Strain and applied load data was acquired through LabView^{TM} on a MacIntosh computer and stored. For each specimen, the stress was determined by dividing the applied load by the initial measured cross-sectional area. All specimens were loaded until catastrophic fracture occurred or an end tab became de-bonded. Of the 12 pure Kevlar and 12 hybrid braided samples which were tested, 10 and 4 were loaded till complete fracture, respectively. Often, before ultimate failure occurred, individual strain gauges became de-bonded and generated erroneous readings. The raw data acquired in these tests were therefore modified to remove the appropriate portion of the strain data. The remaining stress and strain data for each type of specimen (pure Kevlar and carbon/Kevlar hybrid) were then averaged and the results are presented below.

4.1.1. Elastic behavior

For the pure Kevlar (PK) braided samples, the measured longitudinal strain is plotted with respect to the transverse strain (multiplied by -1 for clarity) in Fig. 9. On six of the tested samples, a zero-ninety degree strain gauge was mounted in order to check the recorded readings of the individual longitudinal and transverse gauges. It is believed the discrepancy in measured strain is due to a deteriorated bond of individual gauges on the specimen. For this reason, the averaged measured strains from the zero-ninety gauges will be used as a true reading. The measured Poisson's ratio, which is taken from the initial linear portion of the graph shown in Fig. 9, is reported to be nearly unity. This strongly

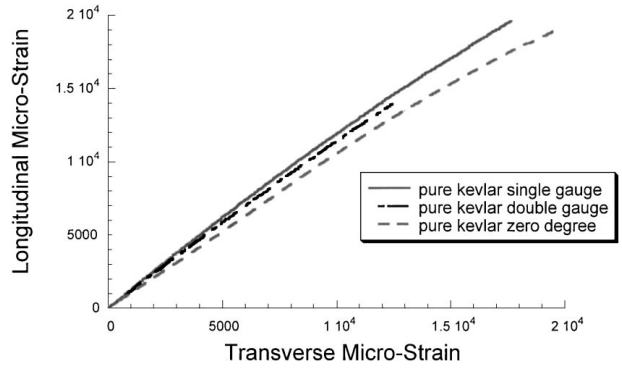

Figure 9 Longitudinal vs. transverse strain in pure Kevlar tension samples.

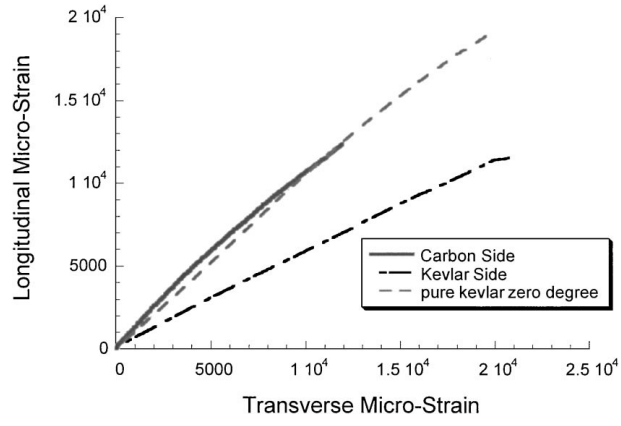

Figure 10 Longitudinal vs. transverse strain in pure Kevlar and carbon/Kevlar hybrid tension samples.

suggests a material elastic response that is dominated by the fiber architecture. The braided composite appears to be behaving in a truss-like fashion. For increased loading, the slightly decreasing, non-linear nature of the Poisson's ratio also suggests a fiber alignment or locking-out effect.

A comparison of the measured Poisson's ratios for the PK and the carbon/Kevlar (CK) hybrid composite samples is shown in Fig. 10. For the CK samples, the initial slope of the curves yields a Poisson's ratio of 1.2 and 0.8 for measurements taken on the carbon and Kevlar sides, respectively. Recall that the Poisson's ratio for the PK samples is near unity. If we assume that an iso-strain condition exists in the longitudinal direction, it is reasonable to believe that the more stiff carbon fibers, which carry the burden of the load, dominate the transverse contraction of the hybrid samples. The presence of the high modulus carbon fibers also produces a more pronounced non-linearity of the Poisson's contraction.

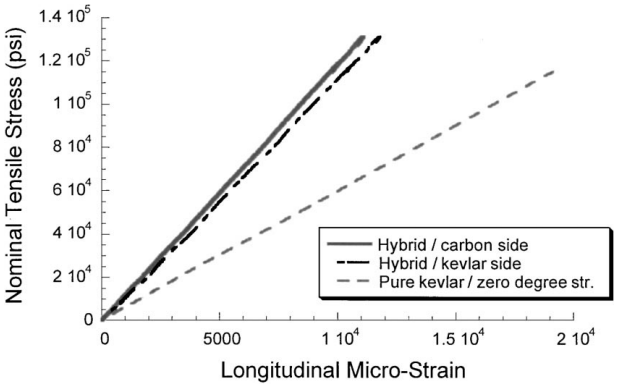

Figure 11 Nominal tensile stress vs. longitudinal strain for pure Kevlar and carbon/Kevlar hybrid tension samples.

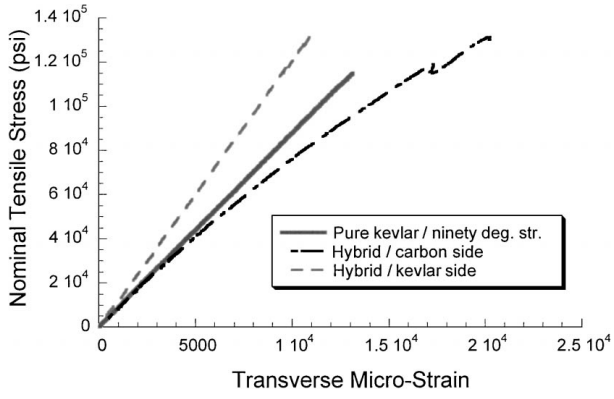

Figure 12 Nominal tensile stress vs. transverse strain in pure Kevlar and carbon/Kevlar hybrid tension samples.

In Fig. 11, the nominal tensile stress is plotted verse the longitudinal strain. For both samples (PK and CK), a linear tensile stress-strain relation is seen to exist. The near equality of the slopes for the carbon and Kevlar sides of the CK sample determines that an iso-strain condition exists in the longitudinal direction. The calculated tensile modulus for the PK sample is 41 Gpa ($6 \times$ E6 psi) while that for the CK sample (averaged) is 74 Gpa ($10.7 \times$ E6 psi).

Finally, examination of the relationship between nominal tensile stress and transverse strain (Fig. 12) supports the conclusion that the transverse contraction of the carbon side of the CK sample is far greater (about 70%) than the Kevlar side. This imbalance in transverse strain must lead to large transverse shearing of the hybrid material. The non-linear transverse contraction behavior of the carbon fiber dominated hybrid is also evident.

4.1.2. Strength and fracture

Linear stress-strain behavior was observed until the ultimate strength was reached, at which time sudden and total fracture occurred. The average ultimate strength of the PK and CK samples are 793 MPa (115 ksi) and 896 MPa (130 ksi), respectively. The average failure strain of the composites are found to be 1.9% and 1.1% for the PK and CK specimens, respectively. Fig. 13a shows typical fractured PK and CK specimens. For all samples, fracture occurred along a near 45 degree shear plane of the material (Fig. 13b).

Observation of the fracture surface near the carbon/Kevlar interface region reveals a dominant growth of cracks in the thickness direction of the sample. Of note is the high crack density in the Carbon tows as seen in Fig. 14a (carbon appears as white). It is believed that near the carbon/Kevlar interface region, the exaggerated difference in transverse strain results in the breaking away of carbon tows from the matrix, carbon tow failure, and final tow pull out (Fig. 14b). A

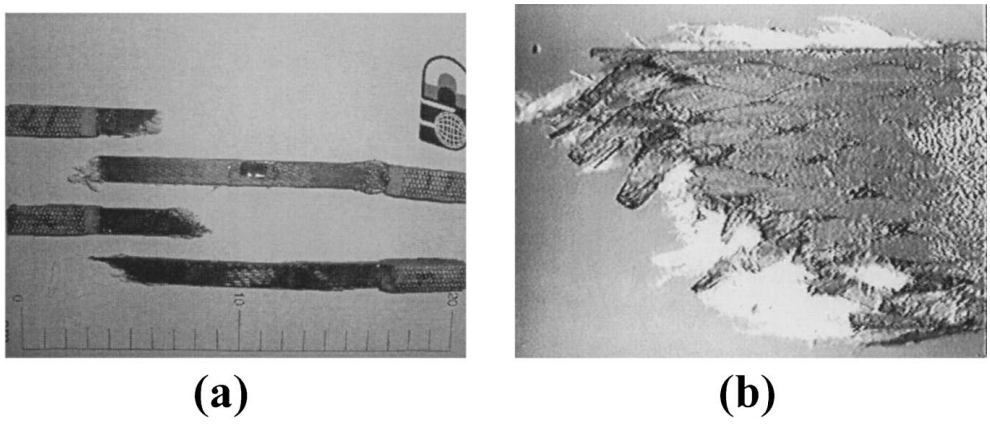

Figure 13 (a) Typical fracture of braided composite specimens and (b) fracture across the shear face in the carbon/Kevlar hybrid sample.

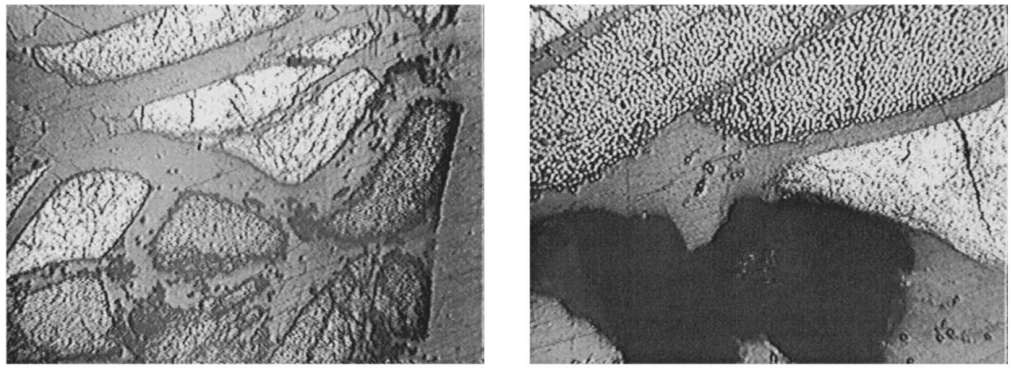

Figure 14 Micrographs showing (a) transverse microcracks within carbon tows and (b) microcracks in the carbon tows with pull-out at the fracture surface.

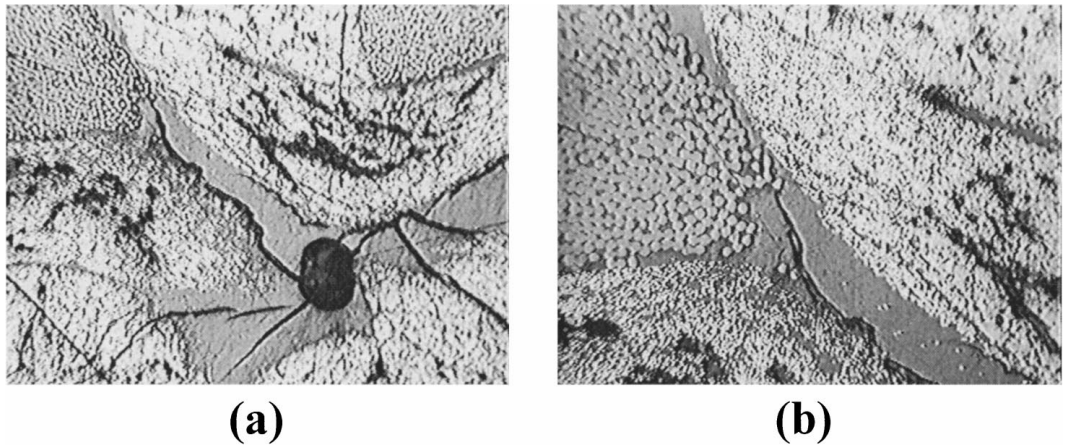

Figure 15 Micrographs showing (a) crack initiation at a void within the inter-tow regions and propagation along the matrix/tow interface, and (b) crack arrest at the Kevlar interface.

likely site of the crack initiation, as with many polymer matrix composites, is voids. Fig. 15a shows several cracks which initiate at an internal void. The cracks appear to dominantly transverse the carbon tows, not the Kevlar tows (Fig. 15b). The characteristics in crack initiation, propagation, and arrest sequence may prove to be an exploitable quality of hybrid composites.

5. Summary and concluding remarks

Textile preforms offer a wide selection of fabrication techniques. It is within this processing science that true control of yarn placement may be realized, resulting in the tailored fabrication of unique micro-structures and the resulting composite performance. In general, the advantages of 3-D Cartesian braiding as a method of preforming include the formation of a delamination resistant structure, the ability to fabricate thick and complex shapes, and single procedure, net-shape preforming. Structural composites formed by this method may be designed to yield the required performance for the intended application.

In this study, Cartesian three-dimensional braiding as a method of preforming for hybrid composites has been investigated. A brief review of 3-D braiding was supplied in order to fully understand the limitations and potentials of the process. The fundamental case of a two-sided hybrid 3-D braid was chosen. Hybrid preforms, along with a corresponding set of non-hybrid preforms for control, were fabricated using a Cartesian braiding method. The preforms were consolidated through a Resin Transfer Molding process and prepared for characterization and mechanical testing. Characterization of the braided hybrid composite specimens included yarn packing and deformation within an assumed unit cell, and measurement of constituent tow fiber volume fraction using digital image analysis.

A comparison study of the elastic performance of Kevlar/epoxy and carbon/Kevlar hybrid composites was carried out. The tension test results show a linear stress-strain relationship for both specimen types within the range of the applied load. The measured tensile modulus for the carbon/epoxy and hybrid composite were found to be 41 Gpa (6.0 Msi) and 74 Gpa (10.7 Msi), respectively. In addition, the Poisson's ratio of near unity for both specimen types strongly suggests a fiber dominated material response. The difference in hybrid composite transverse strain due to the differing constituent fiberous materials is found to be appreciable. It is believed that the discrepancy in Poisson's contraction and fiber stiffness causes the propagation of transverse cracks primarily within the carbon tows and ultimately leads to catastrophic composite failure. The initiation, growth, and arrest of cracks due to the

hybridization of the composite specimens was also observed to occur. Composite ultimate strength and strain to failure were found to be 793 Mpa (115 ksi) and 1.9% for the Kevlar/epoxy sample and 896 Mpa (130 ksi) and 1.1% for the carbon/Kevlar hybrid.

The microstructures and performance of the hybrid composites presented in this study are only a small sampling of the unlimited variations which one may conjure up. For example, a series of braided box structures with carbon fiber/polystyrene filler material as a core may be arranged in a modulated configuration to form selectively reinforced "comb-like" panels. Any of the electrical current-carrying carbon fibers may be utilized as lineal sensors where early breakage of the stiff fibers anticipates complete composite failure. The high Poisson's ratio of the braided network and potentially non-linear stress-strain behavior may be "designed-in" to fit the intended application. Improved transmission and absorption of vibrations within the braided hybrid composite structure is also suggested. There is virtually a world of unfilled uses for these unique structures waiting to be satisfied.

References

1. T.-W. CHOU, in "Microstructural Design of Fiber Composites" (Cambridge University Press, Cambridge, England, 1992) Ch. 6 and 7.
2. D. BROOKSTEIN, US Patent 5,123,458 (Oct. 23, 1994).
3. R. SPAIN and C. BAILEY, US Patent 4,984,502 (Jan. 15, 1991).
4. T. J. IVSAN, US Patent 4,922,798 (May 8, 1990).
5. R. MCCONNELL and P. POPPER, US Patent 4,719,837 (Jan. 19, 1988).
6. M. KIMBARA, M. TSUZUKI, A. MACHII, M. AMANO and K. FUKUTA, in Proceedings of the 4th Japan International SAMPE Symposium, Sep. 25–28, 1995.
7. R. FLORENTINE, US Patent 4,312,261 (January 26, 1982).
8. T.-W. CHOU and P. POPPER, in Proceedings of the Fifth International Conference on Composites Engineering, Las Vegas, Nevada, June 5–11, 1998.
9. T. D. KOSTAR, PhD dissertation, University of Delaware, May, 1998.
10. D. HARTRANF, A. PARVIZI-MAJIDI and T.-W. CHOU, in NASA Contractor Report 198285, February, 1996.
11. C. M. PASTORE and F. K. KO, *Journal of Textile Institute* (81) (1990) 480.
12. P. KISHORE and T.-W. CHOU, *Composite Science and Technology* **53**(3) (1995) 213.
13. M. ITO, PhD dissertation, University of Delaware, May, 1995.
14. L. V. SMITH and S. R. SWANSON, *Composite Science and Technology* **54**(2) (1995) 177.
15. J. HEARLE, J. P. GROSBERG and S. BACKER, "Structural Mechanics of Fibers, Yarns, and Fabrics Vol. 1" (Wiley-Interscience, 1969) p. 80.
16. W. LI, PhD dissertation, North Carolina State University, March 1990.
17. F. K. KO, in Proceedings of Composite Materials Testing and Design (Seventh Conference), ASTM STP 893, Philadelphia, 1986, p. 392.
18. J. M. YANG, C. L. MA and T.-W. CHOU, *Journal of Composite Materials* **20**(5) (1986) 472.
19. J. H. BYUN, PhD dissertation, University of Delaware, May, 1992.
20. S. MOHAJERJASBI, PhD dissertation, Drexel University, 1993.
21. ABUSAFIEH, KALIDINDI and E. FRANCO, in Proceedings of American Society for Composites 9th Technical Conference, Newark, Delaware, 1994, p. 1118.
22. E. FRANCO, M.S. thesis, Drexel University, 1995.
23. J. E. MASTERS, R. L. FOYE, C. M. PASTORE and Y. A. GOWAYED, *Journal of Composites Technology and Research* **15**(2) (1993) 112.

Received 11 June
and accepted 5 October 1999